WALAILAK JOURNAL
http://wjst.wu.ac.th Article

Analytical and Numerical Solutions of Vapor Flow in a Flat Plate Heat Pipe

Mohsen GOODARZI[1], Mohammad Mehdi RASHIDI[1] and Amir Basiri PARSA[2]

[1]*Mechanical Engineering Department, Engineering Faculty, Bu-Ali Sina University, Hamedan, Iran*
[2]*Graduate Student of Mechanical Engineering, Islamic Azad University, Hamedan, Iran*

(Corresponding author; e-mail: mm_rashidi@yahoo.com)

Received: 14 January 2012, Revised: 24 January 2012, Accepted: 13 February 2012

Abstract

In this paper, the optimal homotopy analysis method (OHAM) and differential transform method (DTM) were applied to solve the problem of 2D vapor flow in flat plate heat pipes. The governing partial differential equations for this problem were reduced to a non-linear ordinary differential equation, and then non-dimensional velocity profiles and axial pressure distributions along the entire length of the heat pipe were obtained using homotopy analysis, differential transform, and numerical fourth-order Runge-Kutta methods. The reliability of the two analytical methods was examined by comparing the analytical results with numerical ones. A brief discussion about the advantages of the two applied analytical methods relative to each other is presented. Furthermore, the effects of the Reynolds number and the ratio of condenser to evaporator lengths on the flow variables were discussed.

Keywords: Differential transform method, flat plate heat pipe, homotopy analysis method, laminar viscous flow

Nomenclature

DTM	Differential Transform Method
HAM	Homotopy Analysis Method
$\mathcal{L}$	linear operator of the HAM
$\mathcal{N}$	non-linear operator of the HAM
L	heat pipe length
L_e	evaporator length
L_c	condenser length
p	vapor pressure
P	dimensionless vapor pressure
Re_h	Reynolds number
u	x-component of the vapor velocity
U	dimensionless x-component of the vapor velocity
v	y-component of the vapor velocity
V	dimensionless y-component of the vapor velocity

x	horizontal coordinate
X	dimensionless horizontal coordinate
y	vertical coordinate
Y	dimensionless vertical coordinate
Greek letters	
α	suction to injection velocities ratio
β	condenser to evaporator lengths ratio
μ	vapor viscosity
ρ	vapor density
Subscript	
c	condenser
e	evaporator
ini	initial guess

Introduction

Heat pipes have been widely used in heat transfer applications in the last three decades. Flat plate heat pipes (FPHPs) have been considered due to their advantages such as geometry adaptation, ability for much localized heat dissipation, and the production of an entirely flat isothermal surface in comparison to conventional cylindrical ones. Flat plate heat pipes are effective heat transfer devices in which the phase change of the working fluid in a closed system is used to transfer a large amount of energy instead of inserting a large temperature gradient. They have many industrial applications such as electronic cooling [1,2], spacecraft radiator segments [3,4], and also thermal management in the irradiation facility for boron neutron capture therapy [5-9].

The fluid flow within a heat pipe dealing with the vapor flow in the core region is an important topic in most research studies, because the vapor flow carries energy from the evaporator to the condenser, and characterizes heat transferring limits of the heat pipe. Many researchers have studied one, and two dimensional compressible steady vapor flows in heat pipes [10-13]. The typical cross sections of the vapor core are circular, rectangular, and annular, which are designed based on the particular applications. Heat fluxes were uniformly distributed around the circumference surfaces of the evaporators and condensers except in a few studies [13,14].

Only a few investigators have studied vapor and liquid flow in asymmetrical flat plate heat pipes, which is a more complicated and less understood system compared to the conventional cylindrical ones. Ooijen and Hoogendoorn [4] carried out a two dimensional numerical study for steady incompressible laminar vapor flow in a flat plate heat pipe with an adiabatic top plate for injection Reynolds numbers over a range of $1 < Re < 50$. Their results showed that the velocity profiles were not similar for injection Reynolds number greater than 1. Vafai *et al.* [5] have analytically investigated the liquid and vapor flows as well as overall performance of an asymmetrical flat plate heat pipe. In their case study the vapor space was divided into several channels by vertical wicks. For the heat pipes heated from the top surface, this was quite advantageous for returning condensate and resulted in an enhancement of heat pipe performance. Vafai *et al*. [6] have analyzed the asymmetrical discus heat pipes to develop a comprehensive analytical model. The generalized momentum equation in a porous medium was employed to describe the liquid flow in the discus heat pipe.

Zhu and Vafai [7] carried out 3D analytical and numerical studies for steady incompressible

vapor and liquid flows in an asymmetrical flat plate heat pipe. They showed that for a vapor channel with a width to height ratio greater than 2.5, the 2D model was a good approximation of the 3D one. They accounted for coupling of liquid flow within the top and bottom wicks in addition to the vapor-liquid coupling, and also gravitational effects in their analytical model for the disk shaped heat pipe [15]. This model was used to simulate the disk shaped heat pipe, which was previously tested by North and Avedisian [16] and good agreement was found between the two sets of results. The model was further extended by Zhu and Vafai [17] to vapor flow prediction in the presence of reversal flow.

Wang and Vafai [9] developed two different 1D analytical models for computing transient thermal performance of flat plate heat pipes in startup and shutdown operations. Chen *et al*. [18] studied the transient response of flat plate heat pipes by a simplified and efficient 3D linear model. Xuan *et al*. [19] experimentally and numerically studied the performance of a flat plate heat pipe with a narrow vapor chamber. Sonan *et al*. [20] presented an analytical approach to determine the transient performance of a flat plate heat pipe subjected to heating with multiple electronic components. Koito *et al*. [21] experimentally and numerically analyzed heat transfer in a flat plate heat pipe with a single axisymmetrical heat source. Boukhnouf *et al*. [22] experimentally investigated the performance of a flat plate heat pipe using an IR thermal imaging camera.

Explicit solutions to the nonlinear equations are of fundamental interest. Only a limited number of these problems have precise and standard analytical solutions, so the other ones should be solved using alternative methods. In recent decades many attempts have been made to develop analytical methods for solving such nonlinear equations. One of them is the perturbation method [23], which is strongly dependent on a so called small parameter to be defined according to the physics of the problem. Thus, it is worth developing some new analytical techniques, which are independent of defining a small parameter. In fact the perturbation method cannot provide a simple way to adjust and control the region and rate of convergence of a particular approximated series. Liao introduced the basic idea of homotopy in topology to propose a general analytical method for nonlinear problems, namely the homotopy analysis method [24,25], that does not need any small parameter. This method has been successfully applied to solve many types of nonlinear problems [26-30]. Among the other methods, the homotopy perturbation method (HPM) [31], homotopy analysis method [25], and differential transform method [32] are based on the Taylor series expansion.

Zhou [32] employed the basic idea of DTM for solving linear and nonlinear differential equations in electrical circuit problems. It gives exact values of *n*-th derivative of an analytical function at a point in terms of known and unknown boundary conditions. The differential transform is an iterative procedure for obtaining analytical Taylor series solutions for the corresponding differential equation. Chen and Ho [33] developed this method for partial differential equations and Ayaz [34] applied it to the system of differential equations, and its reliability was demonstrated by Abdel Halim [35]. DTM has been successfully employed to solve many types of nonlinear differential equations [36], and its validity, effectiveness and flexibility have been repeatedly verified.

The purpose of the present work is to use HAM and DTM methods associated with the numerical method to solve governing equations in a flat plate heat pipe to both examine the analytical methods in comparison to each other, and investigate the thermal performance of this typical heat pipe at different thermal, geometrical, and hydraulic conditions.

Problem description and formulation

Figure 1 schematically shows a FPHP, which is usually composed of an evaporator (heating part), and condenser (cooling part). It is assumed that the distance between the two adjacent vertical wicks is sufficiently large, so that it can be assumed that the heat pipe has no vertical wick with a width to height ratio greater than 2.5, hence the 2D analysis is valid [7] in the vapor channel.

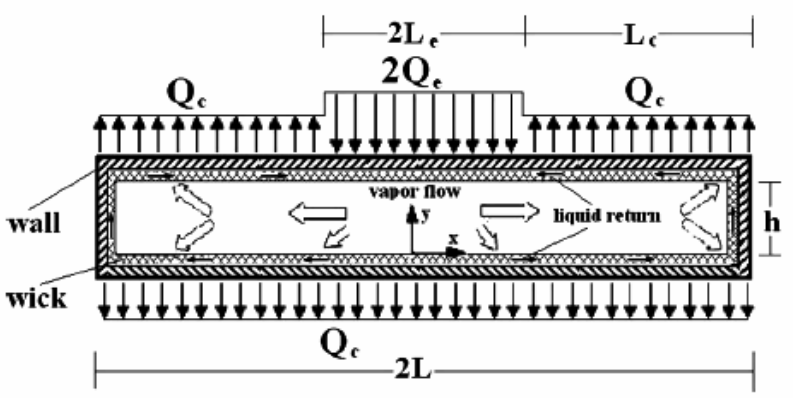

Figure 1 Vapor and liquid flows in a flat plate heat pipe.

Thus evaporation and condensation phenomena are also modeled as uniform injection and suction of vapor at the liquid-vapor interface in the evaporator and condenser parts, respectively. Therefore, dimensionless governing equations for continuity and momentum equations are

$$\frac{\partial U}{\partial X}+\frac{\partial V}{\partial Y}=0, \tag{1}$$

$$U\frac{\partial U}{\partial X}+V\frac{\partial U}{\partial Y} =-\frac{\partial P}{\partial X}+\frac{\mathrm{Re}_h}{\mathrm{Re}_l^{\,2}}\frac{\partial^2 U}{\partial X^2}+\frac{1}{\mathrm{Re}_h}\frac{\partial^2 U}{\partial Y^2}, \tag{2}$$

$$\frac{\mathrm{Re}_h^{\,2}}{\mathrm{Re}_l^{\,2}}\left(U\frac{\partial V}{\partial X}+V\frac{\partial V}{\partial Y}\right) =-\frac{\partial P}{\partial Y}+\frac{\mathrm{Re}_h^{\,3}}{\mathrm{Re}_l^{\,4}}\frac{\partial^2 V}{\partial X^2}+\frac{\mathrm{Re}_h}{\mathrm{Re}_l^{\,2}}\frac{\partial^2 V}{\partial Y^2}, \tag{3}$$

where

$$X=\frac{x}{L},\quad Y=\frac{y}{h}, \tag{4}$$

$$U=\frac{u}{u_1},\quad V=\frac{v}{v_1},\quad P=\frac{p}{\rho u_1^{\,2}},\quad u_1=\frac{L}{h}v_1, \tag{5}$$

$$\alpha=\frac{v_2}{v_1}=\frac{1}{1+2\beta},\quad \beta=\frac{L_c}{L_e}, \tag{6}$$

$$\mathrm{Re}_h=\frac{\rho v_1 h}{\mu},\quad \mathrm{Re}_l=\frac{\rho u_1 L}{\mu}, \tag{7}$$

v_1 and v_2 are the vapor injection and suction velocities in the evaporator and condenser parts, respectively, which are related to each other by applying the conservation of mass in the entire length of the heat pipe:

$$v_1=\frac{Q_e}{\rho L_e h_{fg}},\quad v_2=\frac{Q_c}{\rho(2L_c+L_e)h_{fg}},\quad \frac{v_2}{v_1}=\frac{L_e}{(2L_c+L_e)}, \tag{8}$$

α and β are suction to injection velocities and condenser to evaporator lengths ratios, respectively. Q_e and Q_c are rates of heat transfer in the evaporator and condenser, respectively, which are constant values in the present study. The associated boundary conditions are:

$$\begin{aligned} &U(0,Y)=\frac{\partial V}{\partial X}(0,Y)=0,\\ &U(1,Y)=V(1,Y)=0,\\ &U(X,0)=U(X,1)=0,\\ &V(X,0)=-\alpha,\\ &V(X,1)=\begin{cases}-1 & 0\le X\le \dfrac{1}{1+\beta}\\ \alpha & \dfrac{1}{1+\beta}< X\le 1\end{cases}. \end{aligned} \tag{9}$$

Considering an extended control volume from x = 0 to an arbitrary location in the evaporator section, the conservation of mass flow rate is given by the following equation:

$$\rho(v_1 - v_2)x = \rho\int_0^h u_e(x,y)dy, \tag{10}$$

v_1, and v_2 are constant values, and the left hand side of Eq. (10) is a linear function of x, therefore, the right hand side is also a linear function of the same independent variable, i.e. x, and it can be concluded that:

$$u_e(x,y) = xg'_e(y), \tag{11}$$

the y-component of the velocity vector can be simply obtained from the continuity equation:

$$v_e(x,y) = -g_e(y), \tag{12}$$

and consequently non-dimensional velocity components are:

$$\begin{aligned} U_e(X,Y) &= X\,G'_e(Y), \\ V_e(X,Y) &= -G_e(Y). \end{aligned} \tag{13}$$

Substituting in the momentum equations, the following equations can be derived for non-dimensional pressure gradients:

$$\frac{\partial P_e}{\partial X} = X\left(\frac{G'''_e}{\mathrm{Re}_h} - G'^2_e + G_e G''_e\right), \tag{14}$$

$$\frac{\partial P_e}{\partial Y} = \left(\frac{\mathrm{Re}_h}{\mathrm{Re}_l^{\,2}}G''_e - \frac{\mathrm{Re}_h^{\,2}}{\mathrm{Re}_l^{\,2}}G_e G'_e\right). \tag{15}$$

The right hand side of Eq. (15) is only a function of Y, so differentiating it with respect to X yields:

$$\frac{\partial^2 P_e}{\partial X \partial Y} = 0. \tag{16}$$

Now differentiating Eq. (14) with respect to Y, and considering Eq. (16), the following fourth-order nonlinear ordinary differential equation can be concluded for G_e:

$$G_e^{(4)} + \mathrm{Re}_h(G'''_e G_e - G''_e G'_e) = 0. \tag{17}$$

The associated boundary conditions for this differential equation are:

$$\begin{aligned} &G_e(0) = \alpha, \quad G'_e(0) = 0, \\ &G_e(1) = 1, \quad G'_e(1) = 0. \end{aligned} \tag{18}$$

The pressure distribution along the evaporator can be simply calculated by integrating Eq. (14):

$$\begin{aligned} &P_e(X,Y) - P_e(0,Y) \\ &= \left(\frac{G'''_e}{\mathrm{Re}_h} - G'^2_e + G_e G''_e\right)\frac{X^2}{2}. \end{aligned} \tag{19}$$

With a similar approach, the velocity components, fourth-order nonlinear differential equation with associated boundary conditions, and pressure distribution in the condenser section can be obtained as:

$$\begin{aligned} &U_e(X,Y) = (1-X)G'_e(Y), \\ &V_e(X,Y) = G_e(Y), \end{aligned} \tag{20}$$

$$G_c^{(4)} + \mathrm{Re}_h(G''_c G'_c - G'''_c G_c) = 0, \tag{21}$$

$$\begin{aligned} &G_c(0) = -\alpha, \quad G'_c(0) = 0, \\ &G_c(1) = \alpha, \quad G'_c(1) = 0, \end{aligned} \tag{22}$$

$$\begin{aligned} &P_c(X,Y) - P_c(\frac{1}{1+\beta},Y) \\ &= \frac{1}{2}\left(\frac{G'''_c}{\mathrm{Re}_h} - G'^2_c + G_c G''_c\right) \\ &\left[\left(\frac{\beta}{1+\beta}\right)^2 - (X-1)^2\right]. \end{aligned} \tag{23}$$

Analytical and numerical solutions

Homotopy analysis and differential transform methods can be used to solve the nonlinear Eq. (17) and Eq. (21) with their associated boundary conditions, which were derived for evaporator and condenser parts. Furthermore, governing equations of the vapor flow with corresponding boundary conditions were numerically solved using the well known fourth-order Runge-Kutta method.

HAM solution

The basic ideas of HAM have been described in [25]. In this idea a deformation equation is constructed for approaching an initial guess, which

satisfies boundary conditions, to give a final solution. It is introduced by the following homotopy equation:

$$(1-p)L[G(Y;p)-G_0(Y)]=\hbar pN[G(Y;p)]. \quad (24)$$

Therefore, it needs to define an initial guess $G_0(Y)$, a linear differential operator L, and a nonlinear differential operator N. The initial guesses for the evaporator and condenser parts can be assumed as follows:

$$G_{e0}(Y)=\alpha Y^4-2Y^3+(3-2\alpha)Y^2+\alpha, \quad (25)$$

$$G_{c0}(Y)=-2\alpha Y^4+4\alpha Y^2-\alpha, \quad (26)$$

and from governing nonlinear differential equations, i.e. Eq. (17) and Eq. (21), linear and nonlinear differential operators:

$$L[G_e(Y;p)]=\frac{\partial^4 G_e(Y;p)}{\partial Y^4}, \quad (27)$$

$$L[G_c(Y;p)]=\frac{\partial^4 G_c(Y;p)}{\partial Y^4}, \quad (28)$$

$$N[G_e(Y;p)]=\frac{\partial^4 G_e(Y;p)}{\partial Y^4}+\mathrm{Re}_h\left(\frac{\partial^3 G_e(Y;p)}{\partial Y^3}G_e(Y;p)-\frac{\partial^2 G_e(Y;p)}{\partial Y^2}\frac{\partial G_e(Y;p)}{\partial Y}\right), \quad (29)$$

$$N[G_c(Y;p)]=\frac{\partial^4 G_c(Y;p)}{\partial Y^4}+\mathrm{Re}_h\left(\frac{\partial^2 G_c(Y;p)}{\partial Y^2}\frac{\partial G_c(Y;p)}{\partial Y}-\frac{\partial^3 G_c(Y;p)}{\partial Y^3}G_c(Y;p)\right), \quad (30)$$

Eq. (24) shows that when p changes from 0 to 1, $G(Y;p)$ also changes from $G_0(Y)$ to $G(Y)$, i.e. the analytical solution of nonlinear differential Eq. (17) or Eq. (21). Other details of the solution procedure are only presented for the evaporator section, because they are similar to the condenser's ones. Differentiating Eq. (24) m-times with respect to p, and finally dividing by $m!$, and setting $p = 1$, the following mth-order deformation equation can be obtained:

$$L[G_m(Y)-G_{m-1}(Y)]=\hbar R_m(G_m(Y)), \quad (31)$$

with the corresponding boundary conditions:

$$G_m=G_m'=0, \quad at \;\; Y=0,1, \quad for \quad m\geq 1, \quad (32)$$

where

$$R_m(G_m(Y))=\frac{\partial^4 G_{m-1}(Y)}{\partial Y^4}+\mathrm{Re}_h\left(\sum_{j=0}^{m-1}\frac{\partial^3 G_j(Y)}{\partial Y^3}G_{m-1-j}(Y)-\sum_{j=0}^{m-1}\frac{\partial^2 G_j(Y)}{\partial Y^2}\frac{\partial G_{m-1-j}(Y)}{\partial Y}\right). \quad (33)$$

Considering Eq. (33), the final solution of G_m can be found from Eq. (31):

$$G_m(Y)=G_{m-1}(Y)+\hbar L^{-1}[R_m(G_{m-1})]. \quad (34)$$

The first-order approximation of the HAM solution of $G_e(Y)$ is presented here:

$$G_{e1}(Y)=\frac{1}{2520}(2520\hbar\alpha Y^2-450\hbar\,\mathrm{Re}_h\,Y^2-483\hbar\,\mathrm{Re}_h\,\alpha Y^2+720\hbar\,\mathrm{Re}_h\,\alpha^2Y^2-5040\hbar\alpha Y^2+648\hbar\,\mathrm{Re}_h\,Y^3+1788\hbar\,\mathrm{Re}_h\,\alpha Y^3-1416\hbar\,\mathrm{Re}_h\,\alpha^2Y^3+2520\hbar\alpha Y^4-1890\hbar\,\mathrm{Re}_h\,\alpha Y^4+420\hbar\,\mathrm{Re}_h\,\alpha^2Y^4+252\hbar\,\mathrm{Re}_h\,\alpha Y^5+504\hbar\,\mathrm{Re}_h\,\alpha^2Y^5-378\hbar\,\mathrm{Re}_h\,Y^6+336\hbar\,\mathrm{Re}_h\,\alpha Y^6-140\hbar\,\mathrm{Re}_h\,\alpha^2Y^6+216\hbar\,\mathrm{Re}_h\,Y^7+120\hbar\,\mathrm{Re}_h\,\alpha Y^7-144\hbar\,\mathrm{Re}_h\,\alpha^2Y^7-36\hbar\,\mathrm{Re}_h\,Y^8-153\hbar\,\mathrm{Re}_h\,\alpha Y^8+42\hbar\,\mathrm{Re}_h\,\alpha^2Y^8+36\hbar\,\mathrm{Re}_h\,\alpha Y^9+20\hbar\,\mathrm{Re}_h\,\alpha^2Y^9-6\hbar\,\mathrm{Re}_h\,\alpha^2Y^{10}). \tag{35}$$

Higher order solutions of $G_e(Y)$ are too long to be mentioned here, therefore, they are graphically shown in the figures, which will be described in the following paragraphs.

Note that the series solution contains the auxiliary parameter $\hbar$, which provides a simple way to adjust and control convergence. Liao [25] pointed out that reliable range of $\hbar$ could be defined when no variation of dependent value was observed by $\hbar$ varying. For example, **Figure 2** shows variation of $G_e''(0)$ at Re_h = 0.5 and β = 20 for different orders approximations. It shows that the 10-th order of series has more horizontal segment among the others.

In order to investigate the range of admissible values of the auxiliary parameter $\hbar$, for various quantities of Re_h and β, the curves of $\hbar$ were derived 10th-order approximations. **Figure 3** shows a typical $\hbar$ curve for $G_e''(0)$ meanwhile, for better presentation valid regions are listed in **Table 1**.

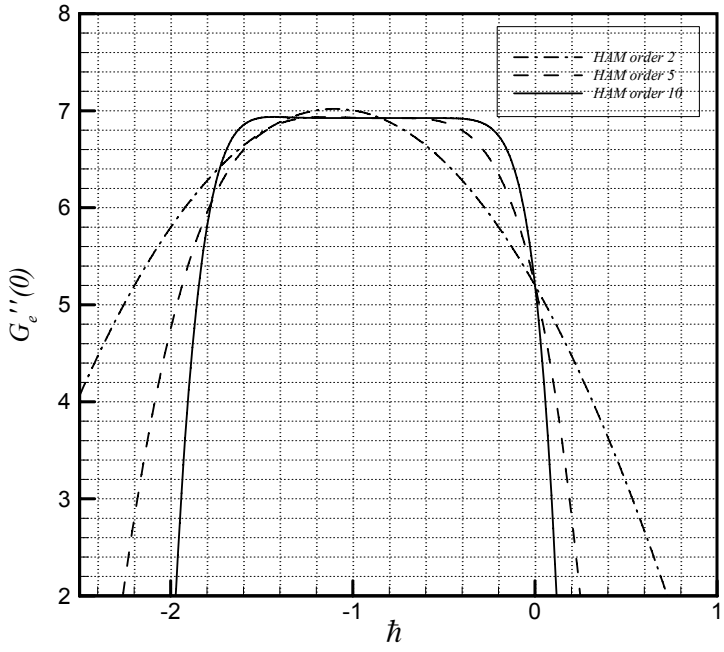

Figure 2 $G_e''(0)$ versus $\hbar$ for different order of HAM approximations with Re_h = 5.0 and β = 2.0.

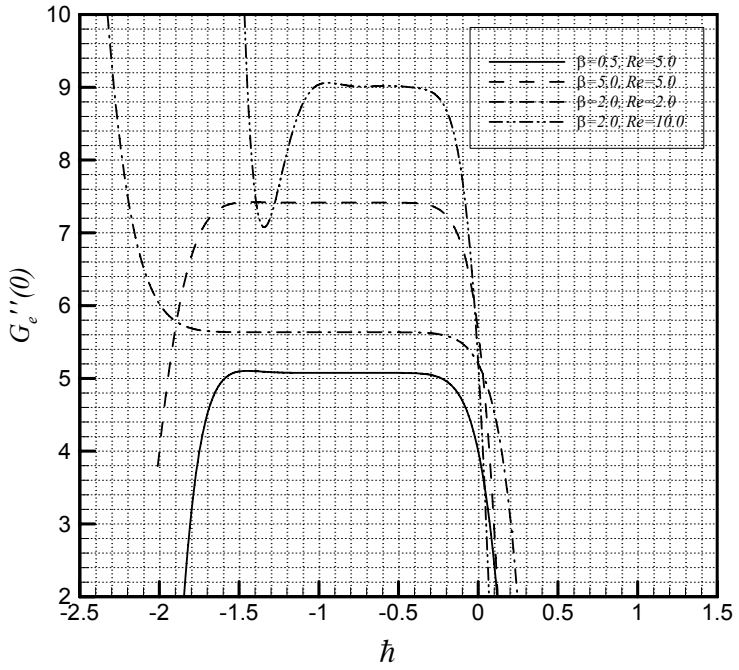

Figure 3 $G_e''(0)$ versus $\hbar$ for 10th-order HAM approximation, for different values of Re_h and β.

Table 1 Admissible and optimal values of $\hbar$ for different values of Re_h and β.

Series solution	Re_h	**5.0**	**5.0**	**2.0**	**10.0**
	β	**0.5**	**5.0**	**2.0**	**2.0**
$G_e(Y)$		$-1.5 < \hbar < -0.1$ $\hbar_{optimal} = -0.8652$	$-1.5 < \hbar < -0.2$ $\hbar_{optimal} = -0.9852$	$-1.8 < \hbar < -0.1$ $\hbar_{optimal} = -0.9875$	$-0.9 < \hbar < -0.1$ $\hbar_{optimal} = -0.5654$
$G_c(Y)$		$-1.4 < \hbar < -0.4$ $\hbar_{optimal} = -1.1347$	$-1.3 < \hbar < -0.2$ $\hbar_{optimal} = -0.6752$	$-1.7 < \hbar < -0.2$ $\hbar_{optimal} = -1.3434$	$-0.6 < \hbar < -0.3$ $\hbar_{optimal} = -0.1884$

In order to choose an optimal value of the auxiliary parameter, averaged residual errors were defined as

$$E_{G,m} = \frac{1}{K}\sum_{i=0}^{K}[N_G(\sum_{j=0}^{m} G_{,j}(j\Delta x))]^2, \tag{36}$$

where $\Delta x = 10/K$ and $K = 20$. Hence, the optimal value of $\hbar$ can be obtained by minimizing E_m:

$$\frac{dE_{G,m}}{d\hbar} = 0. \tag{37}$$

Table 1 also shows obtained optimal values for auxiliary parameter $\hbar$. The following reported results were obtained by optimal values of $\hbar$. It is evident that higher order approximations can better predict the flow field. But what order is the optimal one? It can be defined by plotting some flow variables for several orders of approximations, and defining in what level of order of approximation there would be no difference between the two successive ones.

Figure 4 shows the dimensionless horizontal velocity profiles at X = 0.1 section of the evaporator, and **Figure 5** shows these profiles at X = 0.6 section of the condenser for Re_h = 5.0, β = 2.0, and various orders of HAM in comparison to the numerical results. These figures show that the 10th-order approximation is the minimal required order for this problem.

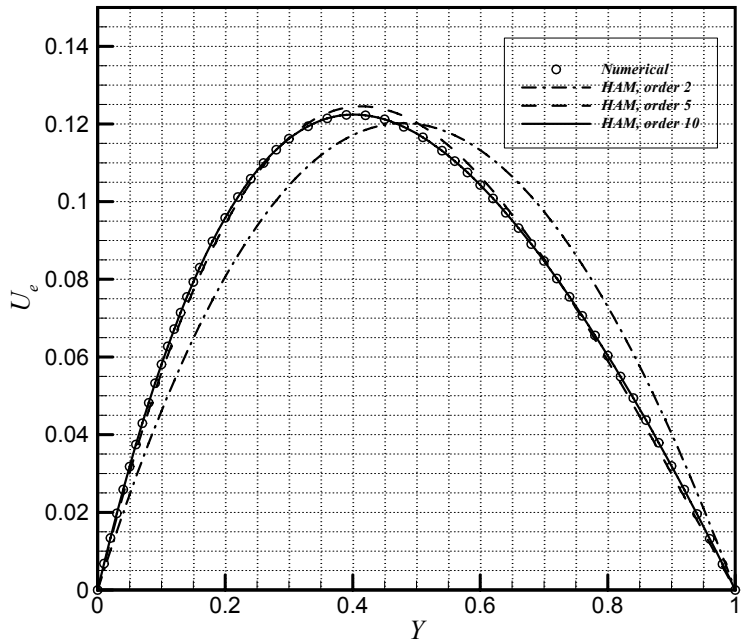

Figure 4 $U_e(Y)$ profiles predicted by Numerical and HAM at X = 0.1, for Re_h = 5.0 and β = 2.0.

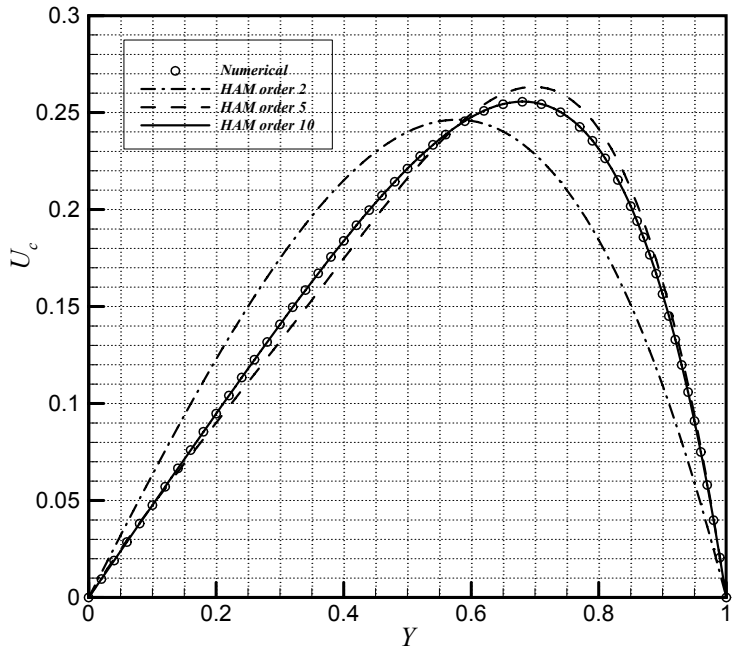

Figure 5 $U_c(Y)$ profiles predicted by Numerical and HAM at X = 0.6, for Re_h = 5.0 and β = 2.0.

DTM solutions

The transformation of the *k*-th derivative of a function in one variable is [36]:

$$F(k)=\frac{1}{k!}[\frac{d^k f(x)}{dx^k}]_{x=x_0}, \tag{38}$$

and the inverse transformation is defined by:

$$f(x)=\sum_{k=0}^{\infty}F(k)(x-x_0)^k. \tag{39}$$

The fundamental mathematical operations performed by the differential transform method are listed in **Table 2**.

Table 2 Fundamental operations of the differential transform method.

Original function	Transformed function
$f(x)=g(x)\pm h(x)$	$F(k)=G(K)\pm H(K)$
$f(x)=cg(x)$	$F(k)=cG(K)$
$f(x)=\frac{d^n g(x)}{dx^n}$	$F(k)=\frac{(k+n)!}{k!}G(k+n)$
$f(x)=g(x)h(x)$	$F(k)=\sum_{l=0}^{k}G(l)H(k-l)$
$f(x)=x^n$	$F(k)=\delta(k-n)=\begin{cases}1, & k=n\\ 0, & k\neq n\end{cases}$

Taking a differential transformation of Eq. (17):

$$\begin{aligned}&(k+1)(k+2)(k+3)(k+4)F(k+4)+\\ &\mathrm{Re}_h[\sum_{k_1=0}^{k}(k-k_1+1)(k-k_1+2)(k-k_1+3)F(k_1)F(k-k_1+3)\\ &-\sum_{k_2=0}^{k}(k-k_2+1)(k-k_2+2)F(k_2)F(k-k_2+2)]=0,\end{aligned} \tag{40}$$

where $F(k)$ is the differential transformation of $G(Y)$. Transformed boundary conditions are

$$\begin{aligned}&F(0)=\alpha, \quad F(1)=0,\\ &F(2)=\gamma, \quad F(3)=\lambda,\end{aligned} \tag{41}$$

where γ and λ are constant values to be evaluated from inverse transformation of the corresponding boundary conditions:

$$\begin{aligned}&G_e(1)=1 \quad \text{or} \quad \sum_{k=0}^{N}F(k)=1,\\ &G_e'(1)=0 \quad \text{or} \quad \sum_{k=0}^{N}(k+1)F(k+1)=0,\end{aligned} \tag{42}$$

and will be obtained by solving the two above equations simultaneously. For example, for Re_h = 5.0, β = 2.0, and N = 20, γ = 3.46292564564, λ = –3.8804238645722, and the DTM solution is:

$$G_e(Y) = 0.2 + 3.46269Y^2 - 3.88042Y^3 + 1025866Y^4 - 0.445753Y^5 + 1.56903Y^6 - 2.035Y^7 + 1.44459Y^8 - 1.7199Y^9 + 2.69985Y^{10} - 2.93146Y^{11} + 2.95835Y^{12} - 3.82772Y^{13} + 4.81457Y^{14} - 5.27187Y^{15} + 6.00586Y^{16} - 7.37008Y^{17} + 8.63033Y^{18} - 9.70934Y^{19} + 11.2828Y^{20}. \quad (43)$$

Eq. (40) associated with boundary conditions Eq. (41) provides a set of algebraic equations, which can be successively computed from $k = 0$ to $k = N$ to find the corresponding successive $F(k)$s. The larger N, the better the prediction of the dependent variable $G(Y)$, but series Eq. (39) asymptotically converges to a certain function. Therefore, like the iterative procedure, which was described for HAM, the minimal value of N can be defined for truncating series Eq. (39). **Figures 6 - 8** show that dimensionless velocity profiles and pressure distribution at $X = 0.1$, 0.6, and $Y = 0.5$, which are compared with numerical results for better comparison. They show that $N = 20$ was the minimal required size of the series Eq. (39).

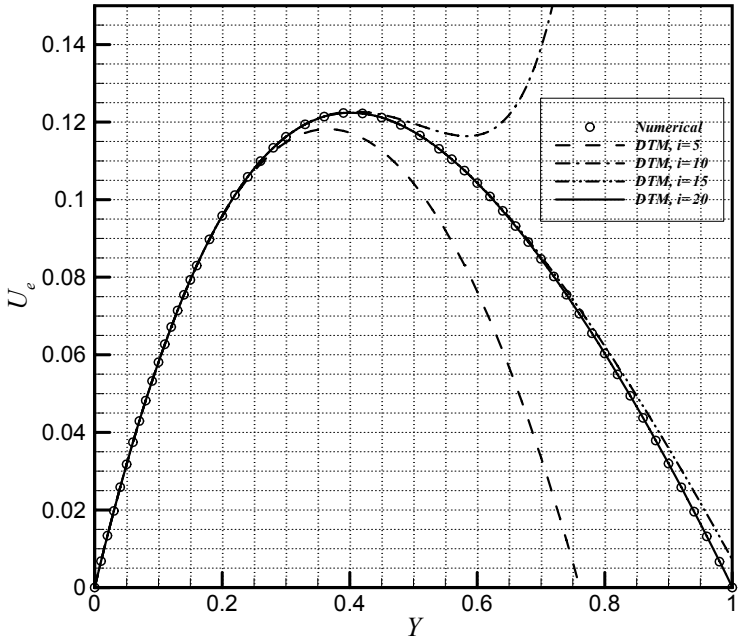

Figure 6 $U_e(Y)$ profiles predicted by Numerical and DTM at $X = 0.1$, for $\mathrm{Re}_h = 5.0$ and $\beta = 2.0$.

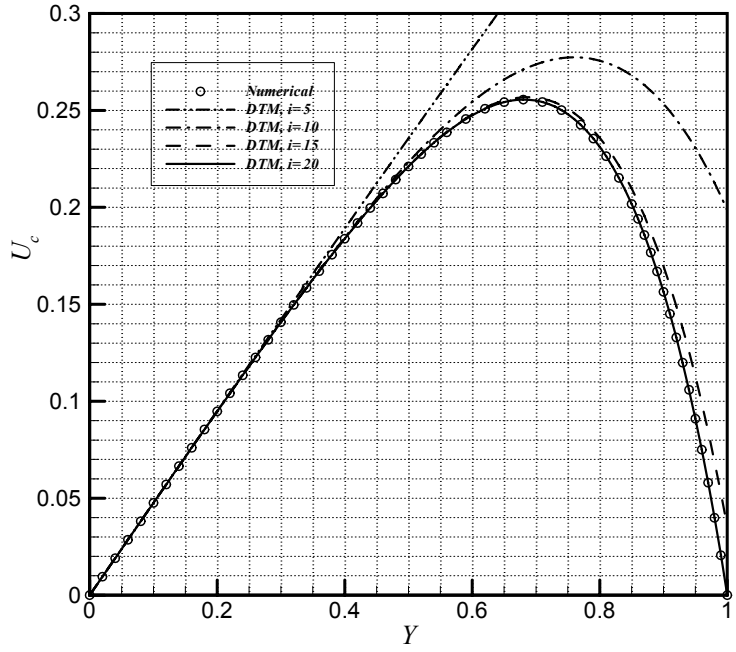

Figure 7 $U_c(Y)$ profiles predicted by Numerical and DTM at $X = 0.6$, for $\mathrm{Re}_h = 5.0$ and $\beta = 2.0$.

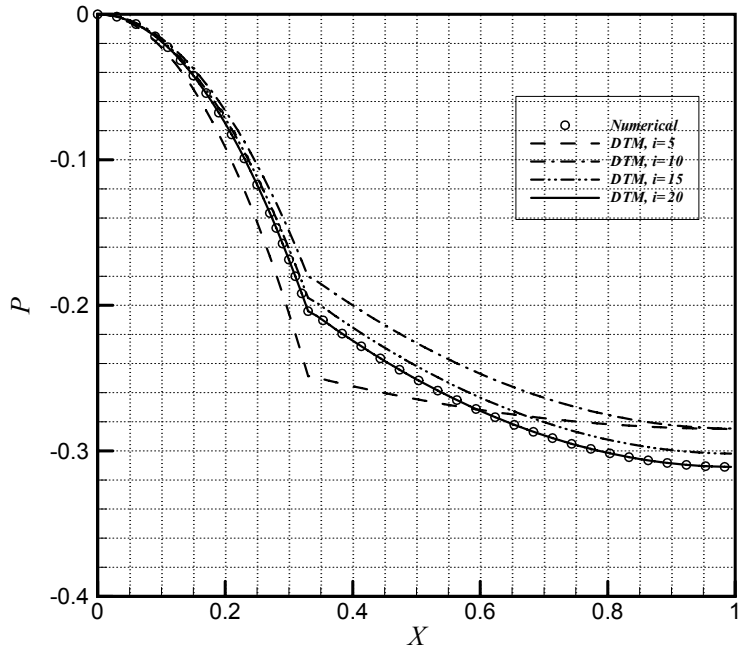

Figure 8 Dimensionless pressure distributions along FPHP at $Y = 0.5$, for $\mathrm{Re}_h = 5.0$ and $\beta = 2.0$.

Results and discussion

All of the already mentioned results should be discussed from an analytical point of view. They showed that both HAM and DTM could analytically solve the nonlinear differential equation with associated boundary conditions, but for HAM an auxiliary parameter, i.e. $\hbar$ must be defined to achieve a consistent solution. Contrary to the HAM, DTM does not need such an auxiliary parameter, and is also simpler than HAM in application, but with a lower order of approximation it may predict an inconsistent solution to the physical problem, see **Figures 6 - 7** for 5th-order of approximation. Hence, there are relative advantages and disadvantages between HAM and DTM, and one should carefully consider the physics of the problem to be solved for applying the better analytical method.

From a physical point of view, the effects of Re_h, and β on velocity profiles and pressure distribution are discussed here. **Figures 9 - 11** represent the effect of Re_h in a typical FPHP with β = 2.0. **Figure 9** shows a horizontal velocity profile at X = 0.1 section of the evaporator, while **Figure 10** shows this velocity at X = 0.6 section of the condenser. These figures show that, the velocity in the evaporator is slightly increased and inclined to the top wall by increasing Re_h, while the velocity in the condenser is significantly decreased with little inclination to the top wall. **Figure 11** shows the pressure distribution along the FPHP. It shows that, the pressure distribution is concave in the evaporator and convex in the condenser parts, which is the main reason for inverse variation of the velocity profiles in these two parts. **Figure 11** shows that, the pressure is slightly decreased in the evaporator, while is significantly increased in the condenser by increasing Re_h. Also, the vapor pressure asymptotically approaches a uniform value (about −0.225) for higher values of Re_h in the condenser.

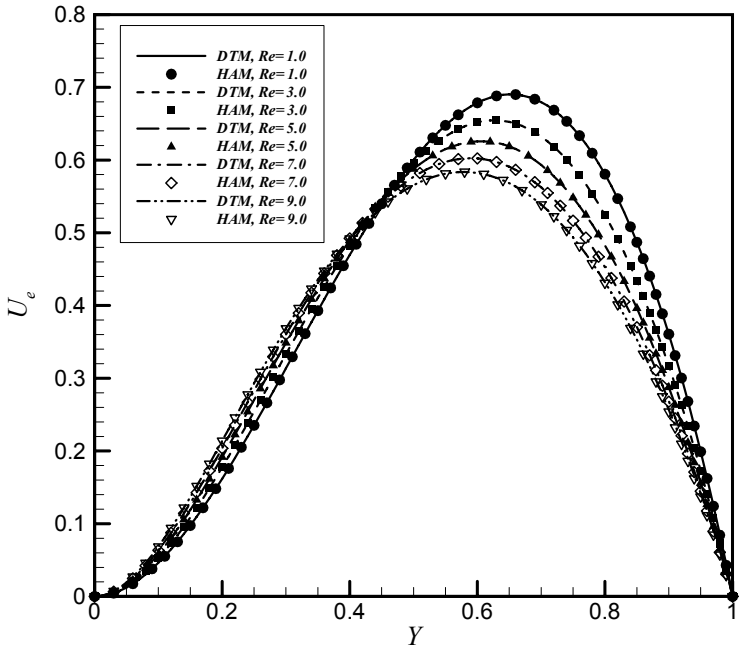

Figure 9 $U_e(Y)$ profiles predicted by HAM and DTM at X = 0.1 and β = 2.0, for several Re_h.

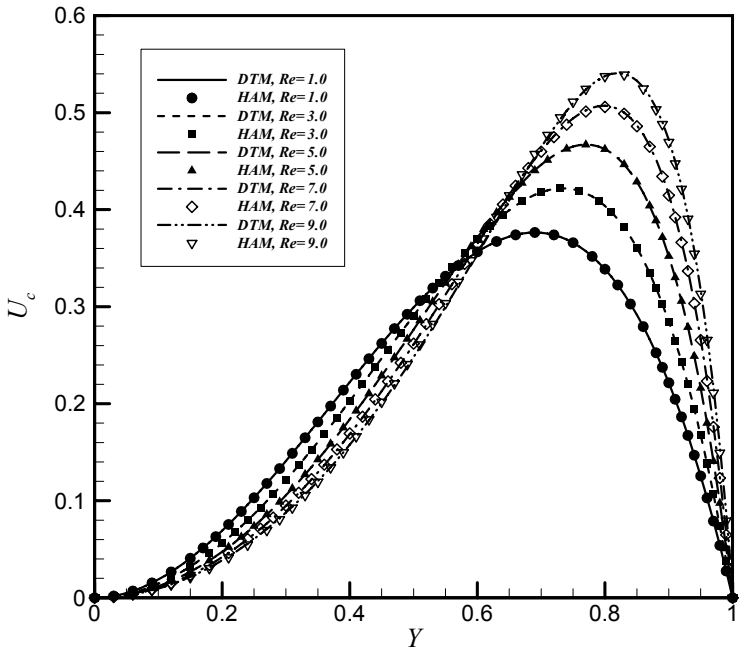

Figure 10 $U_c(Y)$ profiles predicted by HAM and DTM at $X = 0.6$ and $\beta = 2.0$, for several Re_h.

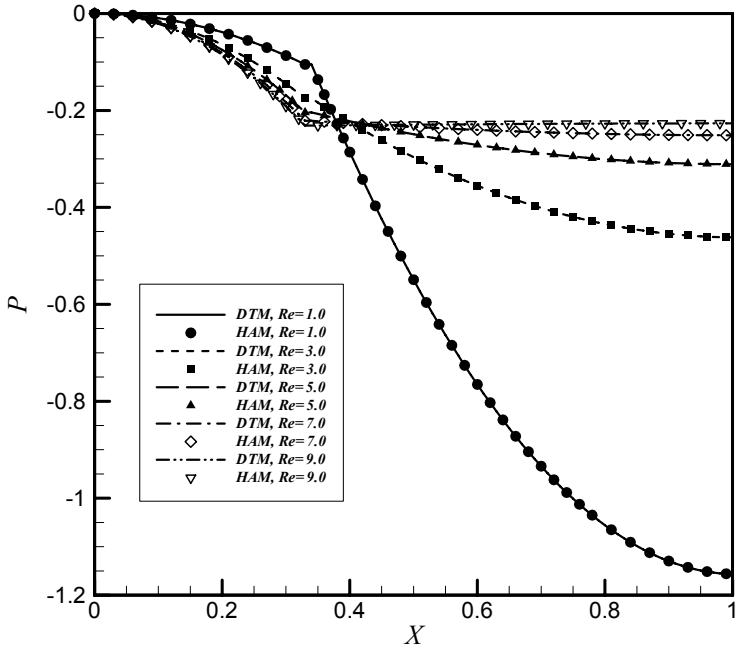

Figure 11 Dimensionless pressure distributions along FPHP at $Y = 0.5$ and $\beta = 2.0$ predicted by HAM and DTM, for several Re_h.

Figures 12 - 13 show x-component velocity profiles at the same mentioned sections of evaporator and condensers, respectively, for Re_h = 5.0 and different values of β. Since Re_h is constant, there are no inclinations in velocity profiles. These figures show that, the velocity at the evaporator section is totally increased by increasing β, while it decreases at the condenser section. Regardless of the value of Re_h, all of the velocity profiles are inclined to the top wall of the FPHP.

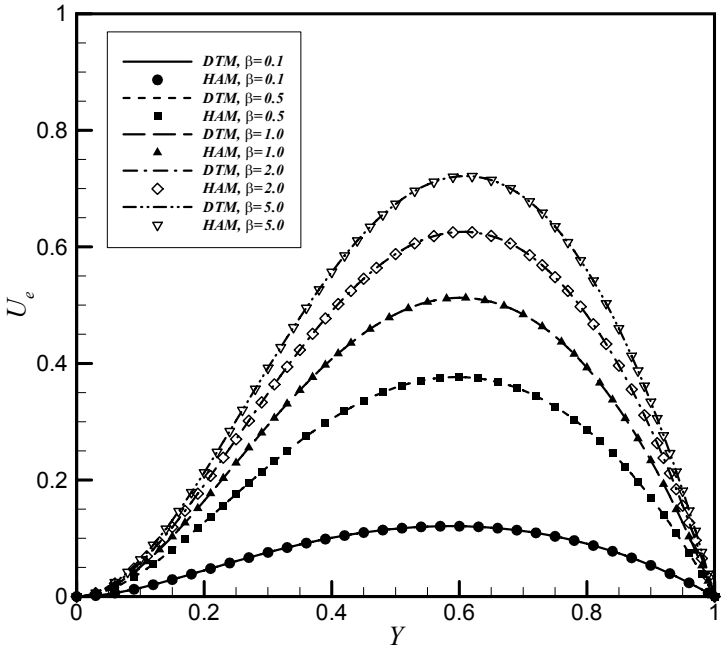

Figure 12 $U_e(Y)$ profiles predicted by HAM and DTM at X = 0.1 and Re_h = 5.0, for several β.

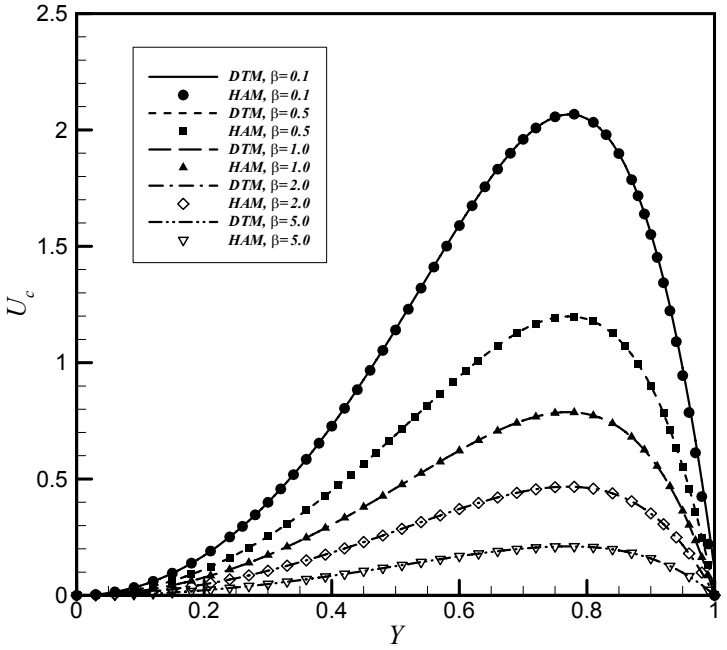

Figure 13 $U_c(Y)$ profiles predicted by HAM and DTM at X = 0.6 and Re_h = 5.0, for several β.

Conclusions

In this paper, the problem of 2D vapor flow in flat plate heat pipes was solved via homotopy analysis and differential transform methods. The validity of the analytical solutions was verified by the numerical results. HAM provides us a convenient way to control the convergence and physical consistency of approximation series by means of an auxiliary parameter $\hbar$, which is a fundamental qualitative advantage of HAM relative to the other methods. It is apparently seen that the HAM is a very powerful and efficient technique for finding analytical solutions for wide classes of nonlinear partial differential equations. On the other hand, the DTM is a simple method with an explicit procedure for solving of non-linear differential equations, but it might lead to physically inconsistent prediction of the problem for lower orders of approximation. From a physical point of view, variation of β and Re_h affect the velocity profiles in the evaporator and condenser sections in an inverse manner, substantially in the condenser part.

References

[1] A Basiulis, H Tanzer and S McCabe. Thermal management of high power PWB's through the use of heat pipe substrates. *In*: Proceedings of the 6th Annual International Electronics Packaging Conference, San Diego, California. 1986, p. 501.

[2] MJ Rightley, CP Tigges, RC Givler, CV Robino, JJ Mulhall and PM Smith. Innovative wick design for multi-source flat plate heat pipes. *Microelectron. J.* 2003; **34**, 187-94.

[3] M Thomson, C Ruel and M Donato. Characterization of a flat plate heat pipe for electronic cooling in a space environment. *In*: Proceedings of the 1989 National Heat Transfer Conference, Heat Transfer in Electronics, Philadelphia, Pennsylvania. 1989, p. 59-65.

[4] H Ooijen and CJ Hoogendoorn. Vapor flow calculations in a flat-plate heat pipe. *AIAA J.* 1979; **17**, 1251-9.

[5] K Vafai, N Zhu and W Wang. Analysis of flow and heat transfer characteristics of an asymmetrical flat plate heat pipe. *Int. J. Heat Mass Tran.* 1992; **35**, 2087-99.

[6] K Vafai, N Zhu and W Wang. Analysis of asymmetrical disk-shaped and flat-plate heat pipes. *ASME J. Heat Tran.* 1995; **117**, 209-18.

[7] N Zhu and K Vafai. Vapor and liquid flow in an asymmetrical flat plate heat pipe: a three dimensional analytical and numerical investigation. *Int. J. Heat Mass Tran.* 1998; **41**, 159-74.

[8] N Zhu and K Vafai. Analytical modeling of the startup characteristics of asymmetrical flat plate and disk-shaped heat pipes. *Int. J. Heat Mass Tran.* 1998; **41**, 2619-37.

[9] Y Wang and K Vafai. Transient characterization of flat plate heat pipes during startup and shutdown operations. *Int. J. Heat Mass Tran.* 2000; **43**, 2641-55.

[10] EK Levy. Theoretical investigation of heat pipes operating at low vapor pressures. *J. Eng. Ind.* 1968; **90**, 547-52.

[11] YM Brovalsky, PI Bystrov and MV Melkinov. The method of calculation and investigation of high temperature heat pipe characteristics taking into account the vapor flow compressibility, friction, and velocity profile. *In*: Proceedings of the 2nd International Heat Pipe Conference, Bologna, Italy. 1976, p. 113-22.

[12] A Faghri. Performance characteristics of a concentric annular heat pipe: part II-vapor flow analysis. *ASME J. Heat Tran.* 1989; **111**, 851-7.

[13] JH Jang. 1988, An Analysis of Startup from the Frozen State and Transient Performance of Heat Pipes, Ph. D. Dissertation. Georgia Institute of Technology, USA.

[14] Y Cao, A Faghri and ET Mahefkey. The thermal performance of heat pipes with localized heat input. *Int. J. Heat Mass Tran.* 1989; **32**, 1279-87.

[15] N Zhu and K Vafai. The effects of liquid vapor coupling and non-Darcian transport on asymmetrical diskshaped heat pipes. *Int. J. Heat Mass Tran.* 1996; **39**, 2095-113.

[16] MT North and CT Avedisian. Heat pipe for cooling high flux/high power semiconductor chips. *J. Electro. Packag.* 1993; **115**, 112-7.

[17] N Zhu and K Vafai. Numerical and analytical investigation of vapor flow in a disk-shaped heat pipe incorporating secondary flow. *Int. J. Heat Mass Tran.* 1997; **40**, 2887-900.

[18] YS Chen, KH Chien, CC Wang, TC Hung and BS Pei. A Simplified transient three-dimensional model for estimating the thermal performance of the vapor chambers. *Appl. Therm. Eng.* 2006; **26**, 2087-94.

[19] Y Xuan, Y Hong and Q Li. Investigation on transient behaviors of flat plate heat pipes. *Exp. Therm. Fluid Sci.* 2004; **28**, 249-55.

[20] R Sonan, S Harmand, J Pellé, D Leger and M Fakès. Transient thermal and hydrodynamics model of flat heat pipe for the cooling of electronics components. *Int. J. Heat Mass Tran.* 2008**; 51**, 6006-17.

[21] Y Koito, H Imura, M Mochizuki, Y Saito and S Torii. Numerical analysis and experimental verification on thermal fluid phenomena in vapor chamber. *Appl. Therm. Eng.* 2006; **26**, 1669-76.

[22] R Boukhanouf, A Haddad, MT North and C Buffone. Experimental investigation of a flat plate heat pipe performance using IR thermal imaging camera. *Appl. Therm. Eng.* 2006; **26**, 2148-56.

[23] AH Nayfeh. *Perturbation Methods*. Wiley, New York, 2000.

[24] SJ Liao. 1992, The Proposed Homotopy Analysis Technique for the Solution of Nonlinear Problems, Ph. D. Thesis: Shanghai Jiao Tong University, China.

[25] SJ Liao. *Beyond Perturbation: Introduction to the Homotopy Analysis Method*. Chapman & Hall/CRC Press, Boca Raton, 2003.

[26] G Domairry and M Fazeli. Homotopy analysis method to determine the fin efficiency of convective straight fins with temperature dependent thermal conductivity. *Commun. Nonlinear Sci. Numer. Simul.* 2009; **14**, 489-99.

[27] MM Rashidi, G Domairry and S Dinarvand. Approximate solutions for the Burger and regularized long wave equations by means of the Homotopy analysis method. *Commun. Nonlinear Sci. Numer. Simul.* 2009; **14**, 708-17.

[28] Z Ziabakhsh, G Domairry and M Esmaeilpour. Solution of the laminar viscous flow in a semi-porous channel in the presence of a uniform magnetic field by using the Homotopy analysis method. *Commun. Nonlinear Sci. Numer. Simul.* 2009; **14**, 1284-94.

[29] MM Rashidi and S Dinarvand. Purely analytic approximate solutions for steady three-dimensional problem of condensation film on inclined rotating disk by Homotopy analysis method. *Nonlinear Anal. R. World Appl.* 2009; **10**, 2346-56.

[30] Z Ziabakhsh and G Domairry. Analytic solution of natural convection flow of a non-Newtonian fluid between two vertical flat plates using Homotopy analysis method. *Commun. Nonlinear Sci. Numer. Simul*. 2009; **14**, 1868-80.

[31] JH He. Homotopy perturbation technique. *Comput. Meth. Appl. Mech. Eng.* 1999; **178**, 257-62.

[32] JK Zhou. *Differential Transformation and Its Applications for Eelectrical Circuits*. Huazhong University Press, Wuhan, China, 1986.

[33] CK Chen and SH Ho. Solving partial differential equations by two dimensional differential transform method. *Appl. Math. Comput.* 1999; **106**, 171-9.

[34] F Ayaz. Solutions of the systems of differential equations by differential transform method. *Appl. Math. Comput.* 2004; **147**, 547-67.

[35] IH Abdel-Halim Hassan. Comparison differential transformation technique with Adomain decomposition method for linear and nonlinear initial value problems. *Chaos Solitons & Fractals* 2008; **36**, 53-65.

[36] A Arikoglu and I Ozkol. Solution of differential-difference equations by using differential transform method. *Int. J. Appl. Math. Comput.* 2006; **181**, 154.